Theoretical studies of effects of 2D plasmonic grating on electrical properties of organic solar cells

Wei E.I. Sha[1], Wallace C.H. Choy[1,], and Weng Cho Chew[1,2,*]*

1 Department of Electrical and Electronic Engineering, the University of Hong Kong, Pokfulam Road, Hong Kong, China.

2 Department of Electrical and Computer Engineering, University of Illinois, Urbana-Champaign, USA.

* chchoy@eee.hku.hk (choy) and wcchew@hku.hk (chew)

Although various optical designs and physical mechanisms have been studied both experimentally and theoretically to improve the optical absorption of organic solar cells (OSCs) by incorporating metallic nanostructures, the effects of plasmonic nanostructures on the electrical properties of OSCs is still not fully understood. Hence, it is highly desirable to study the changes of electrical properties induced by plasmonic structures and the corresponding physics for OSCs. In this work, we develop a multiphysics model for plasmonic OSCs by solving the Maxwell's equations and semiconductor equations (Poisson, continuity, and drift-diffusion equations) with unified finite-difference method. Both the optical and electrical properties of OSCs incorporating a 2D metallic grating anode are investigated. For typical active polymer materials, low hole mobility, which is about one magnitude smaller than electron mobility, dominates the electrical property of OSCs. Since surface plasmon resonances excited by the metallic grating will produce concentrated near-field penetrated into the active polymer layer and decayed exponentially away from the metal-polymer interface, a significantly nonuniform and extremely high exciton generation rate is obtained near the grating. Interestingly, the reduced recombination loss and the increased open-circuit voltage can be achieved in plasmonic OSCs. The physical origin of the phenomena lies at direct hole collections to the metallic grating anode with a short transport path. In comparison with the plasmonic OSC, the hole transport in a multilayer planar OSC experiences a long transport path and time because the standard planar OSC has a high exciton generation rate at the transparent front cathode. The unveiled multiphysics is particularly helpful for designing high-performance plasmonic OSCs.

Organic Photovoltaics XIII, edited by Zakya H. Kafafi, Christoph J. Brabec, Paul A. Lane,
Proc. of SPIE Vol. 8477, 847714 · © 2012 SPIE · CCC code: 0277-786X/12/$18 · doi: 10.1117/12.929498

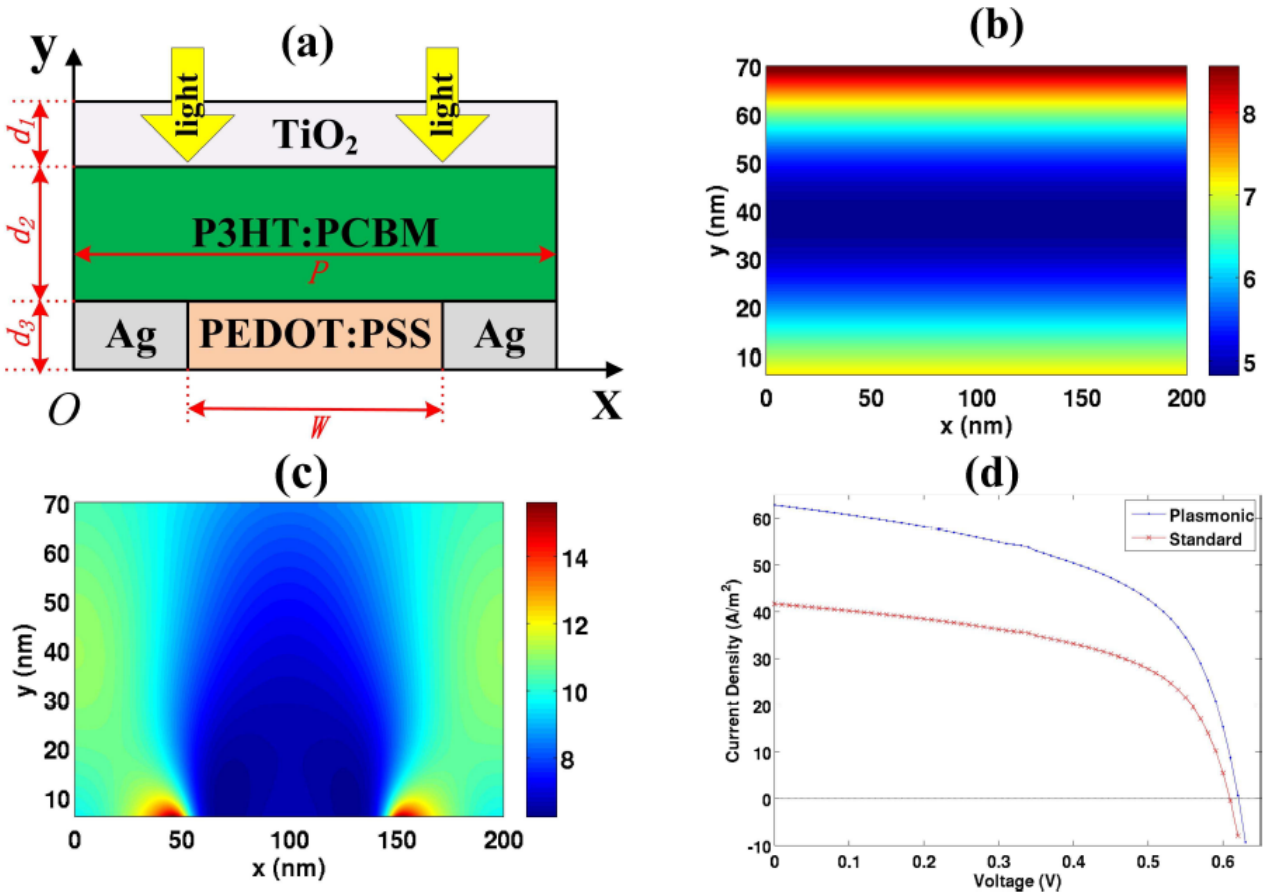

Fig. 1: (a) The schematic unit cell structure of a plasmonic OSC with 2D periodic metallic back grating as an anode. The geometric parameters are set as: d_1 = 30nm, d_2 = 70nm, d_3 = 30nm, W = 100nm, and P = 200nm. The effective bandgap and density of states of the active material P3HT:PCBM is 1.1 eV and 2:5×1019cm^{-3}. The anode of the Ag–PEDOT:PSS–Ag periodic grating is assumed to be an ohmic contact (no injection barrier). The TiO2 cathode layer has an injection barrier of 0.2 eV. (b) The exciton generation rate (×10^{27}) of the standard OSC that replaces the Ag–PEDOT:PSS–Ag grating by a PEDOT:PSS layer. (c) The exciton generation rate (×10^{27}) of the plasmonic OSC. (d) The current density-voltage curves of the plasmonic and standard OSCs under the AM 1.5G light illumination.

Plasmonic	J_{sc} (A/m^2)	V_{oc} (V)	MP (W)	FF	PCE (%)
	62.84	0.62	21.47	0.55	2.15
Standard	J_{sc} (A/m^2)	V_{oc} (V)	MP (W)	FF	PCE (%)
	41.67	0.61	14.03	0.55	1.40

Table 1: The characteristic parameters of plasmonic and standard OSCs involving short-circuit current J_{sc}, open-circuit voltage V_{oc}, maximum power (MP), fill factor (FF), and power conversion efficiency (PCE).

Plasmonic	V (V)	J (A/m^2)	⟨Diss⟩ (%)	⟨Rec loss⟩ (%)
SC	0	62.84	66.96	2.62
MP	0.48	44.73	58.97	14.55
OC	0.62	0	55.47	80.88
Standard	V (V)	J (A/m^2)	⟨Diss⟩ (%)	⟨Rec loss⟩ (%)
SC	0	41.67	66.96	3.18
MP	0.47	30.42	59.19	14.93
OC	0.61	0	55.75	81.91

Table 2: An overview of voltage, current density, exciton dissociation probability (Diss), and recombination loss (Rec loss) at short-circuit (SC), maximum power (MP), and open-circuit (OC) conditions.

Fig. 1(a) shows the schematic pattern of a bulk-heterojunction OSC. The P3HT:PCBM is used as a blend active layer. The cathode and anode of the OSC comprise the transparent and conductive material TiO2 and the Ag–PEDOT:PSS–Ag (lateral) grating layer, respectively. The standard cell, which replaces the Ag–PEDOT:PSS–Ag grating layer by a PEDOT:PSS flat layer, is also modeled. Figs. 1(b) and (c) show the exciton generation rates in the active layer by solving Maxwell's equations. Critically from the standard cell that shows high exciton generation rate near the transparent cathode, the plasmonic cell exhibits very dense exciton generation near the Ag grating anode. Fig. 1(d) shows the corresponding current density-voltage (J-V) curves. Table 1 lists the main characteristic parameters of plasmonic and standard cells. A significant improvement (50% increase) in the short-circuit current can be observed in the plasmonic OSC, which is attributed to the excited surface plasmon resonance for the TM wave and the light trapping effect for the TE wave induced by the metallic grating nanostructure. More intriguingly, the plasmonic grating structure does not reduce the open-circuit voltage of OSCs qualitatively but increases it a bit. The interesting phenomenon seems not to be intuitively understood because more nonuniform and denser exciton generation occurs in the plasmonic cell leading to locally enlarged bimolecular recombination rate proportional to electron and hole concentrations at the initial time. However, the open-circuit voltage depends on the spatially averaged recombination loss at the steady case but not the initial recombination rates. The locally boosted recombination rates at the initial time still can yield smaller recombination loss if the transport path of photogenerated carriers are significantly shortened. In other words, fast collection time of carriers hopping from generation sites to electrodes could reduce recombination loss and thus induces larger open-circuit voltage. For a typical class of organic materials, such as P3HT:PCBM, hole mobility is about one magnitude smaller than electron mobility. Hence, the sweep-out or collection time to electrode is particularly unbalanced for electrons and holes. Having slow collection time, the hole transport will determine the recombination loss of OSCs. On one hand, the grating anode in the plasmonic cell strongly enhances the exciton generation rate nonuniformly distributed near the metal grating due to the exponentially decayed surface plasmon waves away from the Ag/P3HT:PCBM interface. On the other hand, the grating anode facilitates the hole collection with a very short transport path and hopping time. Contrarily, the hole transport in the standard cell experiences a long path because of the high exciton generation rate near the cathode. To demonstrate this point, we calculate the spatially averaged exciton dissociation probability and recombination loss at the steady state as listed in Table 2. The averaged recombination loss can be defined as

$$\langle R_{loss} \rangle = 1 - \frac{\langle U \rangle}{\langle QG \rangle}$$

where $U = QG-(1-Q)R$ is the net generation rate. The recombination loss of the plasmonic cell is smaller than that of the standard cell with larger photovoltages at maximum power and open-circuit conditions.

In conclusion, we investigate the optical and electrical properties of OSCs with a metallic back grating as the anode. Due to favorite hole collections with the short transport path and sweep-out time, the recombination loss of the plasmonic OSC can be smaller than that of the standard cell leading to larger open-circuit voltage. The work establishes a multiphysics framework to seamlessly integrate optical with electrical properties of plasmonic OSCs. The physics unveiled is also useful for designing high-performance organic photovoltaics.

Acknowledgment

The authors acknowledge the support of the grants (Nos. 712010, 711609, and 711511) from the Research Grant Council of the Hong Kong Special Administrative Region, China. This project is also supported in part by a Hong Kong UGC Special Equipment Grant (SEG HKU09) and by the University Grants Council of Hong Kong (No. AoE/P-04/08).